Simplified Analogues of Immucillin-G Retain Potent Human Purine Nucleoside Phosphorylase Inhibitory Activity

Teresa Semeraro,[§] Andrea Lossani,[#] Maurizio Botta,[§] Chiara Ghiron,[†] Reinaldo Alvarez,[#] Fabrizio Manetti,[§] Claudia Mugnaini,[§] Silvia Valensin,[†] Federico Focher,*[,#] and Federico Corelli*[,§]

Dipartimento Farmaco Chimico Tecnologico, Università degli Studi di Siena, Via A. De Gasperi 2, 53100 Siena, Italy, Istituto di Genetica Molecolare, CNR, Via Abbiategrasso 207, 27100 Pavia, Italy, and Sienabiotech S.p.A., Via Fiorentina 1, 53100 Siena, Italy

Received May 10, 2006

A set of deazaguanine derivatives **1**−**3** targeting human purine nucleoside phosphorylase (hPNP) have been designed and synthesized. The new compounds are characterized by the presence of a structurally simplified "azasugar" motif to be more easily accessible by chemical synthesis than previous inhibitors. In the enzymatic assays, some of the new derivatives proved to be able to inhibit hPNP at low nanomolar concentration, thereby showing the same inhibitory potency in vitro as immucillin-H (IMH). Molecular docking experiments revealed a binding mode to hPNP essentially identical to that of IMH. As a result, the lower in vivo activity exhibited by **1d**, compared with that exhibited by IMH, might be ascribed to differences in the pharmacokinetic, rather than pharmacodynamic, profile between these compounds. Derivatives **1a**, **1d**, and **2c** emerged as the most active compounds within this new set and may represent interesting leads in the search for novel hPNP inhibitors.

Introduction

Aberrant T lymphocyte activity is implicated in the development of graft-versus-host disease, in the pathogenesis of diverse autoimmune diseases, in the growth of T cell malignancies, and in the evolution of organ allograft rejection. Suppression of abnormal T cell responses has relied to date on pharmacologic agents that interfere with essential cell surface receptors or metabolic pathways of reactive lymphocytes.[1] However, these agents are usually not selective for T cells, and thus, their use results in host immunosuppression and other serious side effects.

Purine nucleoside phosphorylase (PNP, EC 2.4.2.1) is an enzyme involved in the recycling of nucleosides and deoxynucleosides in cellular remodeling. In the presence of inorganic orthophosphate as a second substrate, PNP catalyzes the cleavage of the glycosidic bond of ribo- and deoxyribonucleosides to generate the purine base and ribose(deoxyribose) 1-phosphate.[2] Although PNP is present in all mammalian cells, T cells are especially sensitive to deficiencies of this enzyme. A rare genetic deficiency of PNP results in a gradual specific loss of T cell function after birth and is associated with significant cellular immunodeficiency.[3] DNA synthesis in other lymphoid and nonlymphoid cells of affected individuals is usually normal, suggesting that inhibition of PNP may provide an effective mechanism for developing specific anticancer drugs that selectively suppress T cell proliferation.[4] Accordingly, several base, nucleoside, and nucleotide analogues have been synthesized and tested as PNP inhibitors, mainly of the human erythrocytes and calf spleen enzymes.[1]

The first inhibitors of PNP were developed by using a structure-based inhibitor design focused on iterative group alignment established from the PNP crystal structures.[5] Following a novel approach based on the identification of the transition-state structure stabilized by the target enzyme, the potent inhibitors (K_i in the picomolar range) immucillin-H (IMH) and immucillin-G (Figure 1) of bovine, malarial, *Mycobacterium tuberculosis*, and human PNPs were identified.[6−10]

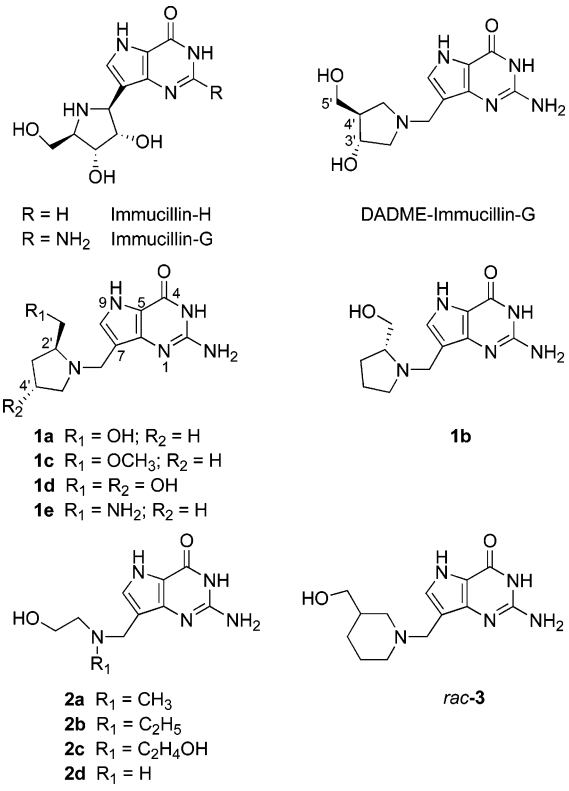

Figure 1. Chemical structures of immucillins and new PNP inhibitors.

IMH is currently in phase I/II clinical trials (as BCX-1777) for the treatment of T cell leukemia.[11] IMH selectively inhibited the in vitro growth of malignant T cell lines in the presence of deoxyguanosine (dGuo) without affecting non-T-cell tumor lines. Activated human peripheral blood T lymphocytes were

* To whom correspondence should be addressed. For F.F.: phone, +39-(0)382-546352; fax, +39-(0)382-422286; e-mail, focher@igm.cnr.it. For F.C.: phone, +39-(0)577-234308; fax, +39-(0)577-234333; e-mail, corelli@unisi.it.

[§] Università degli Studi di Siena.

[#] Istituto di Genetica Molecolare, CNR.

[†] Sienabiotech S.p.A..

10.1021/jm060547+ CCC: $33.50 © 2006 American Chemical Society
Published on Web 08/31/2006

Scheme 1. Preparation of New PNP Inhibitors According to Method A[a]

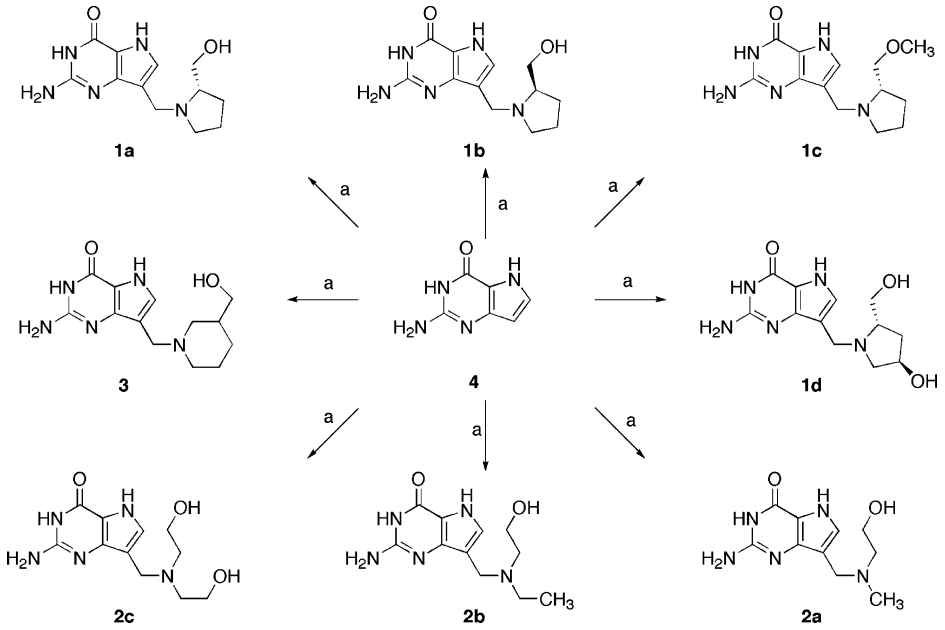

[a] Reagents and conditions: (a) R_1R_2NH, HCl, 30% HCHO, AcONa, H_2O, 95 °C.

also sensitive to inhibition by IMH.[3] Under normal physiologic conditions, dGuo undergoes phosphorolysis by PNP. However, when PNP is inhibited, deoxycytidine kinase (dCK, EC 2.7.1.74) shunts unmetabolized dGuo into dGTP, which accumulates and blocks DNA synthesis through the block of ribonucleotide reductase, the enzyme involved in the supply of the deoxyribonucleotides for DNA synthesis.[1,2]

More recently, the second-generation versions of the immucillins, the DADME-immucillins [namely, 4′-deaza-1′-aza-2′-deoxy-1′-(9-methylene)-immucillins], have been reported to mimic structures further along the phosphorolysis reaction coordinate than the immucillins.[10] The most potent second-generation inhibitor, DADME-immucillin-G (Figure 1), was 8 times more active than the current clinical candidate. This compound was prepared by the efficient coupling of 9-deazaguanine with the hydrochloride salt of (3*R*,4*R*)-3-hydroxy-4-(hydroxymethyl)pyrrolidine via the Mannich reaction.[12] However, the overall synthetic process proved to be rather lengthy, since the hydrochloride salt of (3*R*,4*R*)-3-hydroxy-4-(hydroxymethyl)pyrrolidine must be synthesized from D-xilose in 13 steps.[13] Hence, there is considerable interest in designing and synthesizing DADME-immucillin-G analogues to be more readily accessible by chemical synthesis and with better potential for drug development.

According to our recent interest in phosphorylase inhibitors[14] and in modified nucleosides,[15] we describe herein new PNP inhibitors that share structural features with both immucillin-G and DADME-immucillin-G. In particular, the new compounds (Figure 1) show a hydroxymethyl (or aminomethyl) substituent at the 2-position, instead of 4-position, of the pyrrolidine ring (**1a**−**e**) or lack the whole pyrrolidine ring (**2a**−**d**), which is replaced by an acyclic primary or secondary amine. Finally, compound **3** represents a piperidine homologue bearing the nitrogen atom and the hydroxy group at the same distance from each other as in DADME-immucillin-G.

Results and Discussion

Chemistry. Compounds **1**−**3** were synthesized according to two different methods. In method A, 9-deazaguanine (**4**)[16] was reacted with the appropriate amine hydrochloride in the presence of aqueous formaldehyde and sodium acetate, via a Mannich reaction, at 90−100 °C overnight (Scheme 1). Purification of the reaction mixture by silica gel chromatography gave the final compounds **1a**−**d**, **2a**−**c**, **3** as the corresponding acetate salts in 10−42% yield (Table 1). Both the cyclic and acyclic amines used for the preparation of the new compounds are either commercially available [(*S*)- and (*R*)-prolinol, (*S*)-prolinol methyl ether, *N*-methyl- and *N*-ethylethanolamine, 3-hydroxymethylpiperidine] or can be efficiently prepared in few steps, as in the case of (4*R*)-hydroxy-(*S*)-prolinol.[17] However, the troublesome purification of the products obtained by the Mannich reaction and the low yield of product obtained using primary or hindered secondary amines led us to investigate other methodologies for inserting the amino alcohol chain into compound **4**. Thus, in method B, the protected deazaguanine derivative **5**[16] (Scheme 2) was subjected to Vilsmeier−Haack formylation to give the aldehyde **6** (47% yield), which in turn underwent reductive amination by the action of both primary and secondary amines in the presence of $Na(AcO)_3BH$ as a

Table 1. Physicochemical Data and Human PNP Inhibitory Activity of Compounds **1**−**3**

compd	% yield (method)	mp, °C	hPNP, IC_{50} (nM)[a]	hPNP, K_i (nM)[b]
1a[c]	42 (A)	160−162	4.0 ± 0.3	2.0
1b[c]	39 (A)	152−154	620.0 ± 42.0	316.3
1c	29 (A)	>260	600.0 ± 55.0	306.1
1d	20 (A)	syrup	2.0 ± 0.2	1.0
1e[c]	36[d] (B)	syrup	600.0 ± 50.0	306.1
2a[c]	37 (A)	89−90	60.0 ± 2.5	30.6
2b[c]	10 (A), 55 (B)	syrup	220.0 ± 15.0	112.2
2c[c]	10 (A), 33 (B)	140−141	5.0 ± 0.4	2.5
2d[c]	74 (B)	172−173	20.0 ± 2.0	10.2
3[c]	38 (A)	91−93	4000.0 ± 250.0	2040.8
IMH			3.5 ± 0.2	1.8[e]

[a] IC_{50} values are the average of three determinations. Substrate is 100 μM dGuo. [b] Calculated from the IC_{50} value by using the Cheng−Prusoff equation $K_i = IC_{50}/(1 + D/K_d)$, where D is the concentration of dGuo in the assay (100 μM) and K_d is the K_m of dGuo (104 ± 10 μM) for hPNP. [c] As a diacetate salt. [d] Overall yield for three steps starting from **6** (see Scheme 2). [e] Lit.:[19] $K_i = 3.3 \pm 0.2$ nM.

Scheme 2. Preparation of New PNP Inhibitors According to Method B[a]

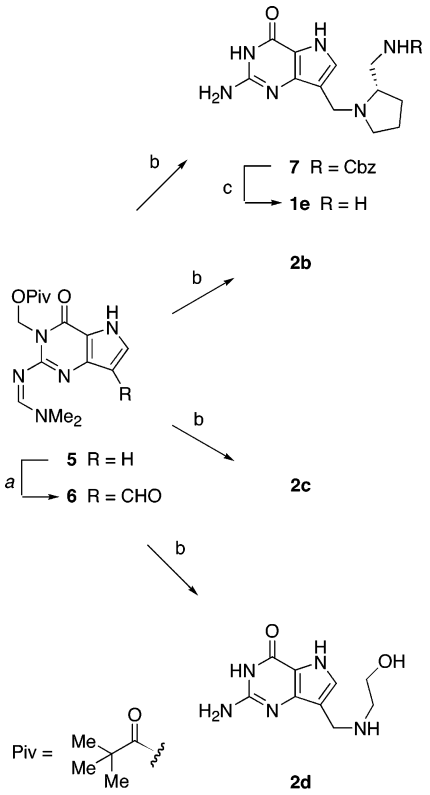

[a] Reagents and conditions: (a) $POCl_3$, DMF; (b) (1) R_1R_2NH, $Na(AcO)_3BH$, DCE, room temp; (2) 1 N NaOH, THF, room temp; (c) H_2, Pd/C, EtOH.

reducing agent to afford, after removal of both pivaloyloxymethyl and dimethylaminomethylene protecting groups by means of 1 N NaOH in THF, the final compounds **2b-d** and **7** in 33−74% overall yield. Commercially available amines (ethanolamine, *N*-methylethanolamine, and diethanolamine) were used in this procedure as well as (*S*)-2-(benzyloxycarbonylaminomethyl)pyrrolidine, which was prepared from (*S*)-1-(*tert*-butoxycarbonyl)-2-aminomethylpyrrolidine[18] by Cbz protection of the primary amino group and deprotection of pyrrolidine nitrogen by standard chemistry (see Supporting Information). Compound **7** was finally converted into **1e** by catalytic hydrogenolysis of the Cbz group (Table 1).

Inhibition of Human Purine Nucleoside Phosphorylase. By following the assay conditions reported in the Experimental Section, the final compounds **1a**−**e**, **2a**−**d**, and **3** were assayed for their ability to inhibit hPNP in vitro, in phosphate buffer in the presence of 100 μM dGuo (K_m concentration) as a substrate, in comparison with the potent inhibitor IMH as a reference compound.[3] The results of these assays are reported in Table 1. Three out of the 10 studied compounds were essentially equipotent to IMH, showing K_i values of 1.0 (**1d**), 2.0 (**1a**), and 2.5 (**2c**) nM, while IMH exhibited a K_i of 1.8 nM. All the other compounds **1**−**3** were 1- to 3-fold less active, their K_i values ranging from 10.2 to 2040.8 nM.

Despite the limited number of compounds tested, some aspects of structure−activity relationship clearly emerge. The presence of a free hydroxy group in the side chain is a fundamental structural feature for hPNP inhibitory activity, since both derivatives **1c** and **1e**, where the OH group has been replaced by a methoxy and a primary amino group, respectively, are 150-fold less active than the corresponding hydroxylated derivative **1a**. This result is in line with the conclusions reported by Lewandowicz et al.[19] about the role of the 5′-hydroxyl (IMH numbering), which is involved in stabilizing an incipient positive charge on the "azasugar" ring that in turn mimics the ribooxacarbenium ion transition state. Thus, the substitution of the 5′-OH by a 5′-NH_2, which is likely to be protonated inside the binding pocket of the enzyme, prevents the stabilization of the cation by lone pairs electrons; however, the decrease of inhibitory activity resulting from alkylation of the 5′-OH (from **1a** to **1c**) is less obvious to be explained only in terms of loss of lone pair interaction,[19] since the methoxy group retains electron-donating properties and in some cases even a methylthio group can answer this purpose well.[19]

The stereochemistry of the hydroxymethyl substituent and the relative distance between the hydroxyl and basic amino group also proved to be crucial for activity. Compound **1b**, having the *R* stereochemistry, was far less active than its *S*-enantiomer **1a**, while the piperidine homologue **3**, where the hydroxyl and basic nitrogen have been moved away by one more carbon atom, was basically inactive. This last result was quite surprising, since in DADME-immucillin-G, the most potent hPNP inhibitor described so far, the pyrrolidine nitrogen and primary OH are spaced out by a three-carbon, not two-carbon, chain. The presence of another hydroxy group on the pyrrolidine ring in the same position and with the same stereochemistry as in DADME-immucillin-G enabled compound **1d** to be 2-fold more potent than **1a** and even slightly more active than IMH.

However, the most striking finding is the substantial activity displayed by simplified, open chain analogues **2a**−**d**. Thus, compound **2d**, where an ethanolamine chain substituted for the hydroxymethylpyrrolidine ring, though 10 times less active than **1d**, nevertheless is still a nanomolar inhibitor of hPNP. Further substitution of the basic nitrogen with short alkyl chains (methyl, ethyl) led to compounds **2a** and **2b**, endowed with reduced activity. Conversely, the insertion on the basic nitrogen of a second hydroxyethyl chain markedly enhanced inhibitory potency, as compound **2c** proved to be basically as potent as **1a**. It is interesting to note that the corresponding 2-deamino analogue of **2c** has been reported to exhibit $K_i = 1.3 \pm 0.1$ nM against hPNP.[19]

hPNP/hdCK Selectivity. Since the anti-T-cell proliferation activity of PNP inhibitors is dependent on the increased level of dGTP pool (because of the block of the catabolic pathway of dGuo, which in turn becomes the substrate of dCK), we decided to investigate whether compounds **1**−**3** might be inhibitors of human dCK. This enzyme, like the herpes simplex virus TK,[20] is characterized by a broad substrate specificity both for the substrate and for the phosphate donor.[21] It can phosphorylate not only dCyd but also 2′-deoxyadenosine (dAdo), 2′-deoxyguanosine (dGuo), and several pyrimidine and purine deoxyribonucleoside analogues (also in the L configuration) modified either in the base or in the sugar ring, such as 2′,3′-dideoxycytidine (ddCyd), 1-β-D-arabinofuranosylcytosine (AraC), 9-β-D-arabinofuranosyladenine (AraA), and 2-chloro-2′-deoxyadenosine (CldA), utilizing various nucleoside triphosphates, also in the L configuration, as phosphate donors.[22] Thus, its inhibition would impair the positive activity of compounds **1**−**3** in vivo. In fact, if inhibited, dCK could not phosphorylate dGuo to dGMP, which once transformed to dGTP blocks the ribonucleotide reductase activity and consequently DNA synthesis. Our studies demonstrated that IMH and the new compounds **1**−**3** are inactive against dCK (data not shown), suggesting possible anti-T-cell proliferation activity in vivo.

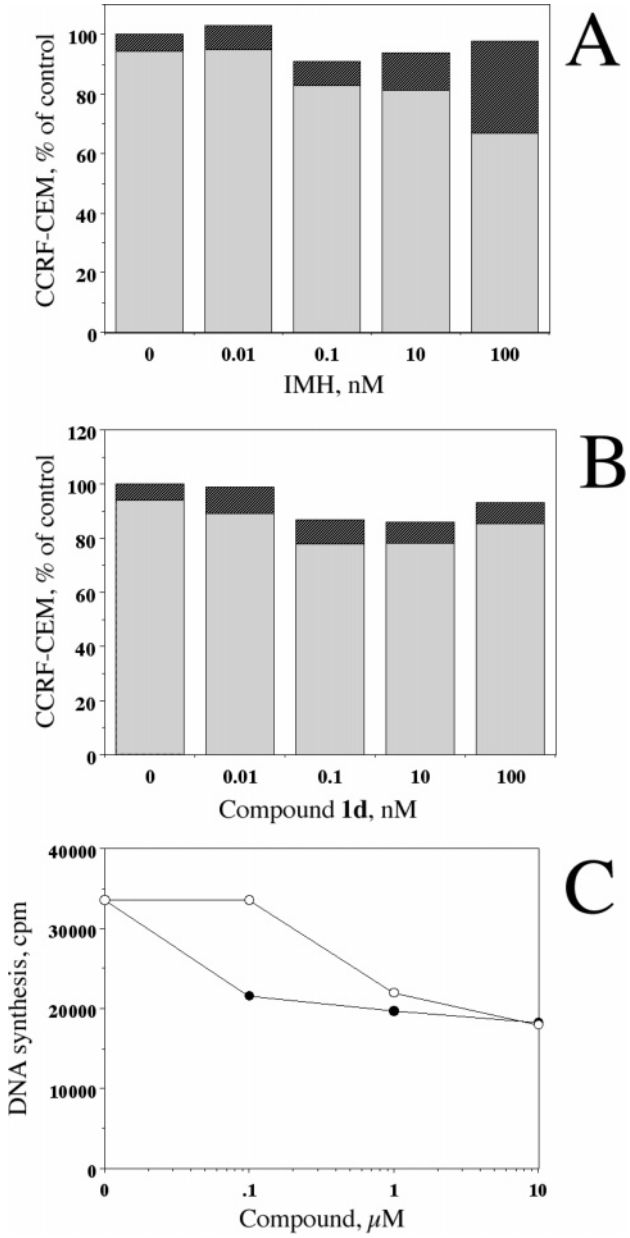

Figure 2. In vivo effect of IMH and **1d** on T cell leukemia cell line CCRF-CEM evaluated as a percentage of living and dead cells after 3 days of treatment with increasing concentrations of IMH (A) and **1d** (B). Cell-growing conditions and method of measurement are described in Experimental Section: (black bar) dead cells; (gray bar) living cells. Panel C shows the effect of increasing concentrations of IMH (black circle) and **1d** (open circle) on DNA synthesis, determined by the [^{3}H]-thymidine incorporation assay described in the Experimental Section.

In Vivo Effect of IMH and 1d on CCRF-CEM. The effects of IMH and **1d** on T cell leukemia cell line CCRF-CEM were evaluated by treating cell cultures with increasing concentrations of IMH and **1d** for 3 days in the presence of 20 μM dGuo, which mimics the extracellular accumulation of this metabolite in human PNP deficiency.[3] In our assay conditions IMH both reduces cell proliferation and increases the percentage of dead cells, whereas **1d** slightly reduces cell proliferation without increasing the percentage of dead cells (parts A and B of Figure 2). Surprisingly, higher concentrations of both compounds do not show any further effect on cell proliferation (data not shown). IMH and **1d** tested up to 100 nM do not inhibit [^{3}H]-thymidine incorporation (data not shown); however, when tested at higher concentrations (up to 10 μM), both compounds weakly inhibited DNA synthesis (Figure 2C).

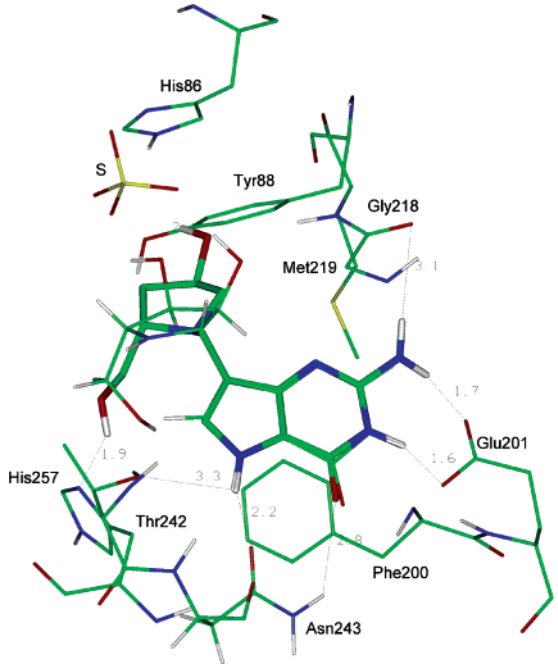

Figure 3. Binding mode and major interactions of **1d** (atom type notation, thick lines) into the active site of PNP. The structure of IMH (atom type notation, thin lines) is also represented for comparison. For the sake of clarity, only a few residues are displayed, with nonacidic hydrogens omitted. Intermolecular hydrogen bonds and electrostatic interactions are represented by dotted black lines. Distances between hydrogen bond and acceptor groups are also shown. S is the sulfate ion labeled as SO4 293H in the pdb file.

If we compare these results with the capability of **1d** to strongly inhibit PNP in vitro and with our molecular docking experiments (see below), it appears that the efficacy of IMH and its derivatives to inhibit T cell growth in vivo might depend on specific cellular uptake. In fact, the disagreement between the in vitro and in vivo effects of **1d** could be explained if we postulate that IMH and its derivatives enter into the cell through a selective transport showing specific K_m values for each compound. Thus, if **1d** shows a higher K_m for this carrier, compared to IMH, it will reach effective intracellular concentrations (similar to those of IMH) only when present in the medium at concentrations higher than IMH.

Antiproliferative Effect on Tumor Cell Lines. The antiproliferative effect of the new compounds was tested on a panel of tumor cell lines: A549 (human lung carcinoma); U87MG, DBTRG-05-MG, T98G (human brain glioblastoma-astrocytoma); DU145 (human prostate carcinoma, metastatic to brain); and HT29 (human colon adenocarcinoma). The MTT assay based on the cleavage of the yellow 3-(4,5-dimethylthiazol-2-yl)-2,5-diphenyltetrazolium bromide into purple formazan crystals by metabolically active cells was used to assess the antiproliferative effect of the compounds, which were tested at concentrations varying from 0.1 nM to 20 μM. Doxorubicin, a well-known antiproliferative anticancer compound, was used as a positive control. The antiproliferative activity of the compounds was calculated as a percentage of remaining viable cells versus control (untreated cells) conditions. Two parameters were used: IG_{50} (the molar concentration of the compounds that produces 50% of the maximum possible antiproliferative response) and the I_{max} (maximum antiproliferative effect). In general the compounds were shown to be ineffective in inhibiting proliferation of all analyzed cell lines. However, for

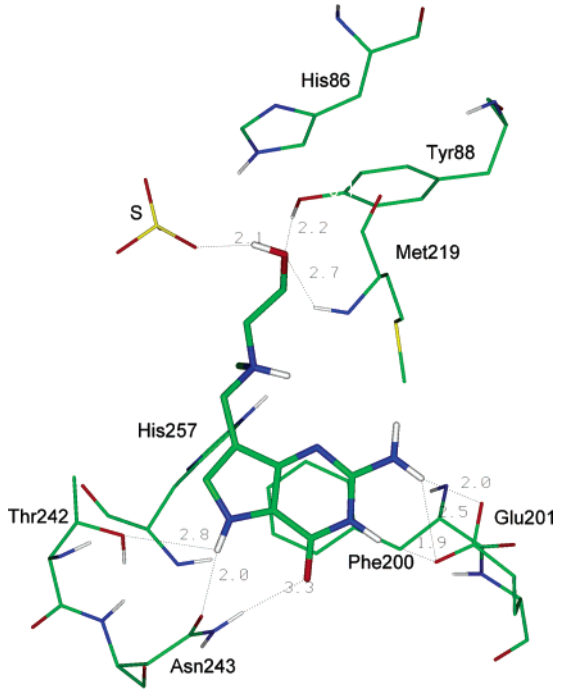

Figure 4. Graphical representation of the major interactions between **2a** (atom type notation, thick lines) and amino acids of the active site of PNP. For the sake of clarity, only a few residues are displayed, with nonacidic hydrogens omitted. Intermolecular hydrogen bonds and electrostatic interactions are represented by dotted black lines. Distances between hydrogen bond and acceptor groups are also shown. S is the sulfate ion labeled as SO4 293H in the pdb file.

one compound (**3**), the IG_{50} on DBTRG-05MG was observed to be in the nanomolar range, but since the I_{max} of this compound was only 20% at 20 μM, we suggest that the overall antiproliferative effect of compound **3** on DBTRG-05MG proliferation is negligible. In conclusion, our findings suggest that the synthesized compounds do not affect non-T-cell tumor line proliferation, thereby supporting the statement that the compounds described are selective inhibitors of human T lymphocytes.[3]

Molecular Modeling. To elucidate the binding mode of the new hPNP inhibitors, a molecular modeling study was carried out taking into consideration derivatives **1a**, **1d**, and **2a** as representatives of the whole set of compounds. Molecular docking simulations showed that the best conformation of **1a** was in an orientation within the PNP binding site very similar to that of the cocrystallized IMH (Figure 3). In detail, the carboxylate terminus of Glu201 was engaged in two hydrogen bonds with both the 3-NH group of the inhibitor bicyclic core and the amino group at position 2. The latter also showed an additional contact with the backbone carbonyl group of Gly218. Moreover, the carbonyl group at position 4 interacted with the side chain NH_2 group of Asn243, while the 9-NH moiety showed a couple of contacts with both the side chain carbonyl group of Asn243 and the hydroxy oxygen of Thr242. Two additional hydrogen bonds involved the 2′- and 4′-hydroxy groups of **1d** that interacted with the imidazole ring of His257 and the hydroxy group of Tyr88, respectively, further stabilizing the complex. Hydrophobic contacts were also found between the side chains of both Tyr88 and Met219 with the C4′−C5′ portion of the cyclic amine, found in an envelope conformation, the C4′ carbon atom being out of the plane of the remaining four atoms (different from the unexpected planar conformation of the crystallographic sugar moiety of IMH). Finally, the Phe200 phenyl ring was parallel to the condensed five-membered ring of the inhibitor, at a distance of about 4.7 Å.

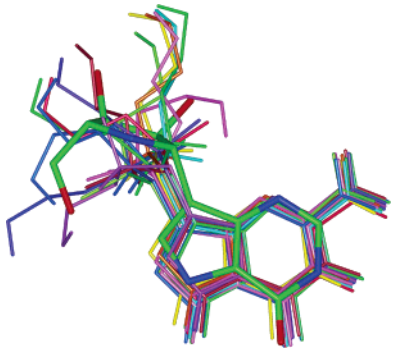

Figure 5. Several poses of **2a** (thin lines) into the PNP binding site are represented in comparison to the orientation of IMH (atom type notation, thick lines), taken from the crystallographic complex coded as 1pf7 in the Brookhaven Protein Data Bank.

On the other hand, the best orientation of **1a** and its contacts with residues of the PNP binding site are very similar to those found for **1d**. The major difference was the loss of the hydrogen bond with Tyr88 due to the lack of the 4′-hydroxy group, counterbalanced by better interactions with Thr242 and the carbonyl group of the Asn243 side chain.

Moreover, the interaction pattern of **2a** was also comparable to that of **1d**, with slight differences (Figure 4). In fact, the total number of hydrogen bonds was maintained, with a different arrangement for contacts involving the 2-amino group. In particular, only one hydrogen of the latter was involved in a bifurcated interaction with the carboxylate group of Glu201, while the second hydrogen atom lacked the interaction with Met219. The remaining four hydrogen bonds were conserved; 3-NH interacted with the Glu201 carboxylate, 4-CO was in contact with the terminal NH_2 of Asn243, and 9-NH was involved in interactions with both the side chain carbonyl group of Asn243 and the hydroxy group of Thr242. The side chain at position 7 of the inhibitor was characterized, in its best conformation, by an orientation that mimicked the 5′-hydroxy group of IMH. The terminal hydroxy group was found to be either a hydrogen bond acceptor, making contact with both the Tyr88 hydroxy group and the Met219 backbone NH group, or a hydrogen bond donor, making contact with one of the oxygen atoms of the sulfate ion. However, because of the high flexibility of the hydroxyethylaminomethyl side chain, it was able to assume many conformations within the binding pocket accommodating the azasugar ring of IMH. As a consequence, the analysis of the preferred poses of the inhibitor within the binding site showed that different conformations of **2a** are characterized by the terminal hydroxy group located in regions of space to mimic the three hydroxy groups of IMH (Figure 5).

Conclusions

Perturbation of T cell population through the inhibition of PNP provides new avenues for the treatment of T-cell-mediated disorders. Accordingly, the development of selective hPNP inhibitors represents an interesting goal in drug design.[28] The inhibitors studied to date, in particular the DADME-immucillins, display high potency and selectivity and are currently in clinical trials. However, the “pseudosugar” substituent at position 7 of the bicyclic moiety is chemically and stereochemically complex so that its preparation by chemical synthesis is not trivial and requires numerous steps. In this paper we have demonstrated that simplified analogues of DADME-immucillin-G, characterized by either cyclic or acyclic substituents readily accessible

by synthesis or even commercially available, retain the ability to selectively inhibit hPNP at low nanomolar concentration without interfering with other enzyme systems, such as hdCK. The most potent compound **1d** proved to be essentially as potent as IMH as a hPNP inhibitor in vitro, although it was 1 order of magnitude less active on the T cell leukemia cell line CCRF-CEM. Since molecular docking experiments with IMH and **1d** confirm our in vitro data, we suggest that the lower in vivo activity exhibited by **1d** compared to IMH might be ascribed to different pharmacokinetic, rather than pharmacodynamic, properties of these compounds. Therefore, although requiring further optimization to improve their in vivo activity, the simplified analogues of the DADME-immucillins here described may represent interesting structural prototypes in the search for new hPNP inhibitors.

Experimental Section

General. Reagents were obtained from commercial suppliers and used without further purifications. According to standard procedures, CH_2Cl_2 was dried over calcium hydride, MeOH and EtOH were dried over Mg/I_2 prior to use, and DMF was bought already anhydrous. Anhydrous reactions were run under a positive pressure of dry N_2 or argon. IR spectra were recorded on a Perkin-Elmer BX FT-IR system. TLC was carried out using Merck TLC plates Kieselgel 60 F254. Chromatographic purifications were performed on columns packed with Merck 60 silica gel, 23−400 mesh, for flash technique. Melting points were taken using a Gallenkamp melting point apparatus and are uncorrected. ^{1}H NMR spectra were recorded with a Bruker AC200F spectrometer at 200 MHz, and chemical shifts are reported in δ values, relative to TMS at δ 0.00 ppm. EI low-resolution MS spectra were recorded using an Agilent series 1100 LC/MSD spectrometer with an electron beam of 70 eV. Elemental analyses (C, H, N) were performed in-house using a Perkin-Elmer 240C elemental analyzer.

Chemistry. General Procedure for the Synthesis of Compounds 1a−d, 2a−c, and 3. Method A. Example: 2-Amino-1,5-dihydro-7-[[(2*S*)-2-(hydroxymethyl)-1-pyrrolidinyl]methyl]-4*H*-pyrrolo[3,2-*d*]pyrimidin-4-one (1a) Acetic Acid Salt. 9-Deazaguanine (**4**) (50 mg, 0.33 mmol) and 30% aqueous formaldehyde (27 μL, 0.41 mmol) were added sequentially to a solution of (*S*)-2-pyrrolidinemethanol (41 μL, 0.41 mmol) and acetic acid (24 μL, 0.41 mmol) in water (2 mL). After the mixture was stirred at 90 °C for 12 h, silica gel (1.0 g) was added to the reaction mixture and volatiles were removed in vacuo. Chromatography on a silica gel column (CH_2Cl_2/MeOH/NH_4OH, 5:3:1) afforded **1a** (42% yield) as a diacetate salt. $[\alpha]^{20}_D$ −24.4 (*c* 1.25, MeOH). ^{1}H NMR (CD_3OD): δ 7.27 (s, 1H), 4.17 (d, J = 13.7 Hz, 1H), 3.94 (d, J = 13.7 Hz, 1H), 3.67 (m, 2H), 3.14 (m, 2H), 2.79 (m, 1H), 1.92 (s, 6H), 1.83 (m, 4H). IR (Nujol) ν_{max} 1674, 1634, 1580, 1525, 1199, 1121 cm^{-1}. MS (electrospray): *m*/*z* 264 [M + 1]. Anal. ($C_{16}H_{25}N_4O_6$) C, H, N.

2,2-Dimethylpropanoic Acid [2-[[(Dimethylamino)methylene]-amino]-4,5-dihydro-7-formyl-4-oxo-3*H*-pyrrolo[3,2-*d*]pyrimidin-3-yl]methyl Ester (6). A solution of **5** (320 mg, 1.0 mmol) in dry DMF (5 mL) was added dropwise to the complex obtained from dry DMF (0.93 mL, 12 mmol) and phosphoryl chloride (1.12 mL, 12 mmol) at 0−5 °C. After being stirred at 100 °C for 3 h, the reaction mixture was cooled, diluted with CH_2Cl_2 (40 mL), and quenched with saturated solution of $NaHCO_3$ (60 mL). The organic layer was separated, washed with brine, dried over anhydrous Na_2SO_4, and evaporated to give a brownish solid. Purification by column chromatography on silica gel (CH_2Cl_2/MeOH, 98:2) gave **6** (165 mg, 47%): mp 253 °C. ^{1}H NMR ($CDCl_3$): δ 10.09 (s, 1H), 8.68 (s, 1H), 7.82 (s, 1H), 6.39 (s, 2H), 3.18 (s, 3H), 3.06 (s, 3H), 1.14 (s, 9 H). IR ($CHCl_3$) ν_{max} 1726, 1668, 1630, 1508, 1214 cm^{-1}. MS (electrospray): *m*/*z* 348 [M + 1]. Anal. ($C_{16}H_{21}N_5O_4$) C, H, N.

General Procedure for the Synthesis of Compounds 2b−d and 7. Method B. Example: 2-Amino-1,5-dihydro-7-[[[2-(hydroxy)ethyl]amino]methyl]-4*H*-pyrrolo[3,2-*d*]pyrimidin-4-one (2d). A solution of **6** (3.47 g, 0.01 mol), ethanolamine (1.83 g, 0.03 mol), and glacial acetic acid (5.4 g, 0.09 mol) in dry 1,2-dichloroethane (50 mL) was stirred at room temperature for 30 min, then treated with $NaBH(AcO)_3$ (6.36 g, 0.03 mol). After being stirred at room temperature for 24 h, the reaction mixture was evaporated to dryness to leave a residue, which was dissolved in THF (60 mL) and 1 N NaOH (60 mL). The reaction mixture was stirred at room temperature for 24 h. Then water (60 mL) and glacial acetic acid (until pH 5) were added and volatiles were removed in vacuo. Purification of the residue by column chromatography on silica gel (CH_2Cl_2/MeOH/NH_4OH, 4:2.5:0.5) yielded compound **2d**, which was dissolved in glacial acetic acid (5 mL) and evaporated in vacuo to provide **2d** (2.54 g, 74%) as the diacetate salt: mp 172−173 °C. ^{1}H NMR (CD_3OD): δ 7.36 (s, 1H), 4.21 (s, 2H), 3.78 (t, J = 4.9 Hz, 2H), 3.11 (t, J = 4.9 Hz, 2H), 1.92 (s, 6H). IR (Nujol) ν_{max} 1702, 1664, 1572, 1332, 1134, 1068 cm^{-1}. MS (electrospray): *m*/*z* 224 [M + 1]. Anal. ($C_{13}H_{21}N_5O_6$) C, H, N.

2-Amino-1,5-dihydro-7-[[(2*S*)-2-(aminomethyl)-1-pyrrolidinyl]-methyl]-4*H*-pyrrolo[3,2-*d*]pyrimidin-4-one (1e). A solution of **7** (0.52 g, 1.0 mmol) in EtOH (20 mL) was hydrogenated in a Parr apparatus for 6 h at room temperature and at the initial pressure of 50 psi in the presence of 10% Pd/C (50 mg). After removal of the catalyst by filtration, the solution was evaporated and the residue was purified by flash chromatography on silica gel (CH_2Cl_2/MeOH/NH_4OH, 7:2:0.5) to afford the pure compound **1e** (0.23 g, 66%) as a syrup. ^{1}H NMR (CD_3OD): δ 7.15 (s, 1H), 3.92 (d, J = 13.5 Hz, 1H), 3.5 (d, J = 13.5 Hz, 1H), 3.17 (m, 1H), 2.98 (m, 2H), 2.47 (m, 1H), 2.05 (m, 1H), 1.92 (s, 6H), 1.68 (m, 4H). IR ($CHCl_3$) ν_{max} 1672, 1578, 1180, 1098 cm^{-1}. MS (electrospray): *m*/*z* 263 [M + 1]. Anal. ($C_{12}H_{18}N_6O$) C, H, N.

Biology. Protein Preparation. Human PNP (hPNP) was purchased from Sigma-Aldrich, Milan (Italy), and deoxycytidine kinase (dCK) was cloned, expressed, and purified as previously described.[23] [^{3}H]-2′-Deoxycytidine ([^{3}H]-dCyd, 18−30 Ci/mmol) was purchased from GE Healthcare Bio-Sciences, Milan (Italy).

Human Purine Nucleoside Phosphorylase Assay. The enzyme was assayed at 37 °C in 25 μL of the following buffer: 50 mM Na phosphate, pH 7.0, and 100 μM dGuo. The resulting mixture was incubated at 37 °C for 0, 10, 20, 30, 60, and 120 min in a plastic reaction tube and then heated for 5 min at 90 °C. The assay tube was centrifuged at 10000*g* for 5 min in a bench centrifuge, and the supernatant (20 μL) was analyzed by HPLC elution on a ChromSep HPLC column SS (150 mm × 4.6 mm). Eluents are as follows: buffer A consisting of 20 mM potassium phosphate buffer, pH 7.5; buffer B consisting of 20 mM potassium phosphate buffer, pH 5.6, 60% methanol. Gradient conditions are as follows: 0 min, 0% buffer B; 40 min, 100% buffer B; flow rate, 1 mL/min. The relative peak areas of deoxyguanosine and guanine (when enzymatically produced) were used to determine the phosphorylase activity. The above assay conditions were also used to determine the inhibitory effect of the tested compounds. To determine IC_{50} values, in these assays 100 μM dGuo was incubated in the presence of different concentrations of the compound. IC_{50} values were calculated by analysis of the areas of the peaks eluted from the column.

2′-Deoxycytidine Kinase Assay. dCK was assayed with a radiochemical method[21] that measures the formation of dCMP from labeled dCyd. The enzyme was incubated at 37 °C in 25 μL of a mixture containing 30 mM HEPES-K^+, pH 7.5, 5 mM $MgCl_2$, 5 mM ATP, 0.5 mM dithiothreitol (DTT), and 1 μM [^{3}H]-dCyd (2200 cpm/pmol). The reaction was terminated by spotting 20 μL of the incubation mixture on a 25 mm DEAE paper disk (DE-81 paper, Whatman). The disk was washed twice in an excess of 1 mM ammonium formate, pH 3.6, to remove unconverted nucleoside, once in distilled water and finally in ethanol. Radioactive dCMP was estimated by scintillation counting in 1 mL of Betamax scintillating fluid (ICN Pharmaceuticals, Segrate, Italy); 1 unit (U) is defined as the amount of enzyme catalyzing the formation of 1 pmol of dCMP in 1 h at 37 °C.

Measurement of Cell Viability and DNA Synthesis. CCRF-CEM (kindly supplied by Dr. O. Turriziani, University "La

Sapienza", Rome, Italy) were cultured at 37 °C in RPMI-1640 medium containing 10% heat inactivated FCS, 2 mM L-glutamine, and gentamicine (50 μg/mL). For cell viability studies CCRF-CEM were grown in a 96-well microplate at 1×10^6 cells/mL (200 μL/well) for 72 h in the presence of 20 μM dGuo and different concentrations of IMH and TS-105 (10 pM to 100 nM). Then an amount of 20 μL of the cell suspension was removed from the well and mixed with 20 μL of trypan blue solution (0.5% in PBS). Both viable cells (not stained) and dead cells (blue stained) were then counted. Each point was done in triplicate, and the number of cells counted in each well is the average of four determinations. To the remaining 180 μL, 1 μC of [^{3}H]thymidine was added. After 1 h of incubation at 37 °C, an amount of 40 μL of the cell suspension was spotted in quadruplicate on GF/C filters (Whatman Italia, Milan, Italy). Filters were then washed three times in an excess of 5% (v/v) trichloroacetic acid to remove the unincorporated nucleoside and washed twice in ethanol and finally dried. Acid precipitable radioactivity was measured as described above.

Malignant Cell Lines. The human glioblastoma cell lines (U87MG, DBTRG-05-MG, and T98G), the human colon carcinoma (HT29), and the human prostate carcinoma-metastatic to brain (DU145) were obtained from ICLC (Interlab Cell Line Collection, Genova, Italy). DU145, U87MG, and DBTRG-05-MG were cultured in RPMI 1640. HT29 was cultured in McCoys and the T98G in MEM. In all the medium types were added 10% heat-inactivated FBS, Glutamax, and penicillin/streptomycin.

Cell Proliferation Assay on Non-T-Cell Tumor Cell Lines. Cell proliferation was measured by a colorimetric assay based on formazan production from tetrazolium salt. Cells were grown in 96-well plates at 3000 (DU145, HT29), 2500 (DBTRG-05-MG), and 2000 cells/well for U87MG cells, all in a total volume of 100 μL of medium.

After cell adhesion to the plates, the medium was changed and the compounds were added in different dilutions to a final volume of 100 μL. Following 4 days of incubation, the medium was replaced by 100 μL of fresh medium without serum and cell vitality was assessed using MTT [3-(4,5-dimethylthiazol-2-yl)-2,5-diphenyltetrazolium bromide]: to each well, an amount of 10 μL of MTT solution was added, and the cells were further incubated for 4 h at 37 °C. The blue MTT-formazan product was solubilized by addition of 100 μL of a buffer consisting of 2-propanol, Triton X-100, and HCl. The absorbance was measured at 570 nm using a Victor III spectrophotometer. The antiproliferative activity was calculated as a percentage of remaining viable cells versus control (untreated cells). The result for each experimental condition is the mean of three to four replicate wells.

The activity of the compounds was assessed in concentration response using 0.1 nM, 1 nM, 5 nM, 10 nM, 50 nM, 100 nM, 500 nM, 1 μM, 5 μM, 10 μM, and 20 μM (50 μM only for **1c** and **1d**). Compound efficacy was evaluated using I_{max} (maximum antiproliferative effect) and IG_{50} (the molar concentration of the compounds that produces 50% of the maximum possible antiproliferative response). For the antiproliferative compounds, IG_{50} values were obtained with a nonlinear regression sigmoid concentration response curve using the program Excel Fit.

Molecular Modeling. All calculations and graphical manipulations were performed on SGI computers (Origin 300 server and Octane workstations) using the software package MacroModel/BatchMin[24] equipped with the OPLS-AA force field.[25] A computational protocol, consisting of molecular docking, conformational analysis, and energy minimization procedures, has been applied to evaluate the interaction pathways between the new compounds and PNP. For this purpose, among many crystallographic three-dimensional structures of PNP (in the apo form or in complex with inhibitors) available in the Brookhaven Protein Data Bank, we have chosen the complex between the human PNP and IMH (entry 1pf7, 2.6 Å resolution)[26] for subsequent calculations. To create the initial coordinates for the docking studies, the crystallographic water molecules and sulfate ions were removed from the PNP−IMH complex, with the exception of the sulfate ion labeled as SO4 293 that, in the crystal structure, interacted by a hydrogen bond with the 5′-hydroxy group of IMH. Hydrogen atoms were added to their idealized positions at pH 7.0 using InsightII (version 2000.1) biopolymer software.[27] The atomic partial charges for the enzyme were taken from the OPLS-AA force field.

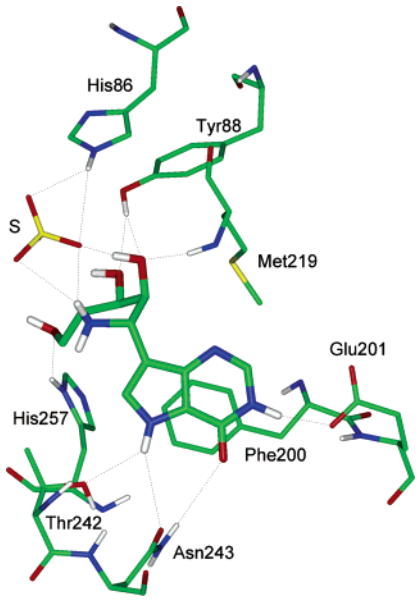

Figure 6. Representation of the best conformation of IMH (atom type notation, thick lines) as found by molecular docking and energy minimization calculations. Both orientation and hydrogen bond network of IMH are also found in the PNP−IMH crystallographic structure. Intermolecular hydrogen bonds and electrostatic interactions are represented by dotted black lines. S is the sulfate ion labeled as SO4 293H in the pdb file.

Inhibitor structures were built using MacroModel, with the amino nitrogen in the protonated form. Atomic partial charges were assigned with the ESP method and MNDO approximation. In the present study, the computational step corresponding to the molecular docking approach is simplified, since the topography of the enzyme active site, as well as the binding mode of many enzyme inhibitors, is known. Thus, the docking problem is essentially reduced to locate the possible orientations/conformations of the inhibitors within the active site of the enzyme.

The reliability of the docking approach has been preliminarily tested on the prediction of the binding geometry of IMH into the binding site of PNP (Figure 6). As a result, docking simulations were able to identify, among all the theoretical lowest-energy structures that were found, PNP−INH complexes with structures very similar to the experimental X-ray structure. In fact, the orientation of INH and the network of hydrogen bonds observed in the X-ray structure was maintained in the output docking geometries. Moreover, the root-mean square deviation (calculated on the heavy atoms of 26 residues of the binding site, in addition to the heavy atoms of IMH) between the crystallographic structure and the minimun energy conformation was 0.8 Å. These considerations led us to hypothesize that the computational approach can be considered as a reliable modeling procedure to be applied for finding the orientations and interactions of ligands inside the catalytic cavity of PNP.

Once the reliability of the docking procedure was tested, it was also applied to the new inhibitors. In detail, IMH was extracted from the PNP−IMH complex and replaced by **1a**, **1d**, or **2a**. A random orientation was chosen for each inhibitor within the binding site, with the 9-NH group pointing toward His86, the 4-CO toward Ser33, and the 5′-OH toward Glu201. The corresponding complexes were then submitted to a statistical conformational search consisting of 10 000 steps of the statistical pseudo Monte Carlo (SPMC) method involving all the rotatable bonds of the inhibitors. It is important to note that the conformational mobility of the active site residues was not a complicating factor because it has been

reported that these residues undergo only minor structural changes upon the binding of IMH to the active site.[26] Moreover, the BatchMin command MOLS was applied to allow for rotation and translation of the inhibitor into the active site, with a maximum value for the random rotational angle set to 180° and a maximum allowed translational movement of 3.0 Å at each step. Because of the large number of atoms in the model, to optimize the PNP−inhibitor complexes obtained by the flexible docking and conformational search procedures, the following additional constraints had to be imposed. A subset, comprising only the inhibitor and a shell of residues possessing at least one atom 5 Å from any of the inhibitor atoms, was created and subjected to energy minimization. The inhibitor and all the amino acid side chains of the shell were unconstrained during energy minimization to allow for reorientation and proper hydrogen-bonding geometries and van der Waals contacts. All the atoms not included in the above-defined subset were fixed, but their nonbond interactions with all the relaxing atoms have been calculated.

Energy minimization of the complexes was performed using the Polak−Ribiere conjugate method until the derivative convergence was 0.01 kcal $Å^{-1}$ mol^{-1}. Solvation conditions were simulated using a continuum approach (GB/SA).

Acknowledgment. We are grateful to Dr. Vern L. Schramm (Department of Biochemistry, Albert Einstein College of Medicine of Yeshiva University) for providing a sample of immucillin-H for biological tests. Financial support from Project FIRB:RBAU01LSR4_001 is gratefully acknowledged (F.F.). T.S. thanks Sienabiotech S.p.A. for a fellowship.

Supporting Information Available: The experimental procedure and analytical data for the remaining compounds described in this paper. This material is available free of charge via the Internet at http://pubs.acs.org.

References

(1) Bzowska, A.; Kulikowska, E.; Shugar, D. Purine nucleoside phosphorylases: properties, functions, and clinical aspects. *Pharmacol. Ther.* **2000**, *88*, 349−425.

(2) Friedkin, M.; Kalckar, H. M. Desoxyribose-1-phosphate: I. The phosphorolysis and resynthesis of purine desoxyribose nucleoside. *J. Biol. Chem.* **1950**, *184*, 437−448.

(3) Kicska, G. A.; Long, L.; Hörig, H.; Fairchild, C.; Tyler, P. C.; Furneaux, R. H.; Schramm, V. L.; Kaufman, H. L. Immucillin H, a powerful transition-state analog inhibitor of purine nucleoside phosphorylase, selectively inhibits human T lymphocytes. *Proc. Natl. Acad. Sci. U.S.A.* **2001**, *98*, 4593−4598.

(4) Giblett, E. R.; Ammann, A. J.; Wara, D. W.; Sandman, R.; Diamond, L. K. Nucleoside-phosphorylase deficiency in a child with severely defective T-cell immunity and normal B-cell immunity. *Lancet* **1975**, *1*, 1010−1013.

(5) Ealick, S. E.; Babu, Y. S.; Bugg, C. E.; Erion, M. D.; Guida, W. C.; Montgomery, J. A.; Secrist, J. A., III. Application of crystallographic and modeling methods in the design of purine nucleoside phosphorylase inhibitors. *Proc. Natl. Acad. Sci. U.S.A.* **1991**, *88*, 11540−11544.

(6) Kline, P. C.; Schramm, V. L. Purine nucleoside phosphorylase. Catalytic mechanism and transition-state analysis of the arsenolysis reaction. *Biochemistry* **1993**, *32*, 13212−13219.

(7) Kline, P. C.; Schramm, V. L. Pre-steady-state transition-state analysis of the hydrolytic reaction catalyzed by purine nucleoside phosphorylase. *Biochemistry* **1995**, *34*, 1153−1162.

(8) Miles, R. W.; Tyler, P. C.; Furneaux, R. H.; Bagdassarian, C. K.; Schramm, V. L. One-third-the-sites transition-state inhibitors for purine nucleoside phosphorylase. *Biochemistry* **1998**, *37*, 8615−8621.

(9) Evans, G. B.; Furneaux, R. H.; Gainsford, G. J.; Hanson, J. C.; Kicska, G. A.; Sauve, A. A.; Schramm, V. L.; Tyler, P. C. 8-Azaimmucillins as transition-state analogue inhibitors of purine nucleoside phosphorylase and nucleoside hydrolases. *J. Med. Chem.* **2003**, *46*, 155−160 and references therein.

(10) Evans, G. B.; Furneaux, R. H.; Lewandowicz, A.; Schramm, V. L.; Tyler, P. C. Synthesis of second-generation transition state analogues of human purine nucleoside phosphorylase. *J. Med. Chem.* **2003**, *46*, 5271−5276 and references therein.

(11) Bantia, S.; Ananth, S. L.; Parker, C. D.; Horn, L. L.; Upshaw, R. Mechanism of inhibition of T-acute lymphoblastic leukemia cells by PNP inhibitor BCX-1777. *Int. Immunopharmacol.* **2003**, *3*, 879−887.

(12) Evans, G. B.; Tyler, P. C. Process for Preparing Pyrrolidine Nucleoside Analogs via Mannich Reaction as Inhibitors of Nucleoside Phosphorylases and Nucleosidases. Patent WO 2004069856, August 19, 2004.

(13) Evans, G. B.; Furneaux, R. H.; Tyler, P. C.; Schramm, V. L. Synthesis of a transition state analogue inhibitor of purine nucleoside phosphorylase via the Mannich reaction. *Org. Lett.* **2003**, *5*, 3639−3640.

(14) Corelli, F.; Botta, M.; Lossani, A.; Pasquini, S.; Spadari, S.; Focher, F. Microwave-assisted synthesis and biological evaluation of novel uracil derivatives inhibiting human thymidine phosphorylase. *Farmaco* **2004**, *59*, 987−992.

(15) (a) Mugnaini, C.; Botta, M.; Coletta, M.; Corelli, F.; Focher, F.; Marini, S.; Renzulli, M. L.; Verri, A. Research on L-nucleosides. Synthesis and biological evaluation of a series of L- and D-2′,3′-dideoxy-3′-[tris(methylthio)methyl]-β-pentofuranosyl nucleosides. *Bioorg. Med. Chem.* **2003**, *11*, 357−366. (b) Paolini, L.; Petricci, E.; Corelli, F.; Botta, M. Microwave-assisted C-5 iodination of substituted pyrimidinones and pyrimidine nucleosides. *Synthesis* **2003**, 1039−1042. (c) Petricci, E.; Radi, M.; Corelli, F.; Botta, M. Microwave-enhanced Sonogashira coupling reaction of substituted pyrimidinones and pyrimidine nucleosides. *Tetrahedron Lett.* **2003**, *44*, 9181−9184.

(16) Furneaux, R. H.; Tyler, P. C. Improved syntheses of 3*H*,5*H*-pyrrolo-[3,2-*d*]pyrimidines. *J. Org. Chem.* **1999**, *64*, 8411−8412.

(17) Reed, M. W.; Adams, A. D.; Nelson, J. S.; Meyer, R. B., Jr. Acridine- and cholesterol-derivatized solid supports for improved synthesis of 3′-modified oligonucleotides. *Bioconjugate Chem.* **1991**, *2*, 217−225.

(18) Slaitas, A.; Yeheskiely, E. Synthesis and hybridization of novel chiral pyrrolidine based PNA analogue. *Nucleosides Nucleotides Nucleic Acids* **2001**, *20*, 1377−1379.

(19) Lewandowicz, A.; Taylor Ringia, E. A.; Ting, L.-M.; Kim, K.; Tyler, P. C.; Evans, G. B.; Zubkova, O. V.; Mee, S.; Painter, G. F.; Lenz, D. H.; Furneaux, R. H.; Schramm, V. L. Energetic mapping of transition state analogue interactions with human and *Plasmodium falciparum* purine nucleoside phosphorylases. *J. Biol. Chem.* **2005**, *280*, 30320−30328.

(20) (a) Spadari, S.; Maga, G.; Focher, F.; Ciarrocchi, G.; Manservigi, R.; Arcamone, F.; Capobianco, M.; Carcuro, A.; Colonna, F.; Iotti, S.; Garbesi, A. L-Thymidine is phosporylated by herpes simplex virus type-1 thymidine kinase and inhibits viral growth. *J. Med. Chem.* **1992**, *35*, 4214−4220. (b) Maga, G.; Focher, F.; Wright, G.; Capobianco, M.; Garbesi, A.; Bendiscioli, A.; Spadari, S. Kinetic studies with N^2-phenylguanines and with L-thymidine indicate that herpes simplex virus type-1 thymidine and thymidylate kinases share a common active site. *Biochem. J.* **1994**, *302*, 279−282. (c) Spadari, S.; Ciarrocchi, G.; Focher, F.; Verri, A.; Maga, G.; Arcamone, F.; Iafrate, E.; Manzini, S.; Garbesi, A.; Tondelli, L. 5-Iodo-2′-deoxy-L-uridine (L-IdU) and (*E*)-5-(2-Bromovinyl)2′-deoxy-L-uridine (L-BVdU): selective phosphorylation by herpes simplex virus type 1 thymidine kinase, antiherpetic activity and cytotoxicity studies. *Mol. Pharmacol.* **1995**, *47*, 1231−1238. (d) Spadari, S.; Maga, G.; Verri, A.; Bendiscioli, A.; Tondelli, L.; Capobianco, M.; Colonna, F.; Garbesi, A.; Focher, F. Lack of stereospecificity of some cellular and viral enzymes involved in the synthesis of deoxyribonucleotides and DNA: Molecular basis for the antiviral activity of unnatural L-β-nucleosides. *Biochimie* **1995**, *77*, 861−867.

(21) Verri, A.; Focher, F.; Priori, G.; Gosselin, G.; Imbach, J.-L.; Capobianco, M.; Garbesi, A.; Spadari, S. Lack of enantiospecificity of human deoxycytidine kinase. Relevance for the activation of β-L-deoxycytidine analogs as antineoplastic and antiviral drugs. *Mol. Pharmacol.* **1997**, *51*, 132−138.

(22) Verri, A.; Montecucco, A.; Spadari, S.; Gosselin, G.; Boudou, V.; Imbach, J.-L.; Focher, F. L-ATP is recognised by some cellular and viral enzymes: does the chance drive enzymatic enantioselectivity? *Biochem. J.* **1999**, *337*, 585−590.

(23) Roy, B.; Verri, A.; Lossani, A.; Spadari, S.; Focher, F.; Aubertin, A. M.; Gosselin, G.; Mathe, C.; Perigaud, C. Enantioselectivity of ribonucleotide reductase: a first study using stereoisomers of pyrimidine 2′-azido-2′-deoxynucleosides. *Biochem. Pharmacol.* **2004**, *68*, 711−718.

(24) *MacroModel*, version 8.5; Schrodinger, L.L.C.: Portland, OR, 2003.

(25) Jorgensen, W. L.; Maxwell, D. S.; Tirado-Rives, J. Development and testing of the OPLS all-atom force field on conformational energetics and properties of organic liquids. *J. Am. Chem. Soc.* **1996**, *118*, 11225−11236.

(26) de Azevedo, W. F., Jr.; Canduri, F.; Marangoni dos Santos, D.; Pereira, J. H.; Dias, M. V.; Silva, R. G.; Mendes, M. A.; Basso, L. A.; Palma, M. S.; Santos, D. S. Structural basis for inhibition of human PNP by immucillin-H. *Biochem. Biophys. Res. Commun.* **2003**, *309*, 917−922.

(27) *InsightII*, version 2000.1; Accelrys, Inc.: San Diego, CA, 2003.

(28) Montgomery, J. A. Purine nucleoside phosphorylase: A target for drug design. *Med. Res. Rev.* **1993**, *13*, 209−228.

JM060547+